Spectral Dependence and Wavelength Selectivity in Heterogeneous Photocatalysis. I. Experimental Evidence from the Photocatalyzed Transformation of Phenols

ARTICLE *in* THE JOURNAL OF PHYSICAL CHEMISTRY B · NOVEMBER 2000

Impact Factor: 3.3 · DOI: 10.1021/jp001927o

3 AUTHORS, INCLUDING:

Alexei V Emeline
Saint Petersburg State University
75 PUBLICATIONS **2,201** CITATIONS
SEE PROFILE

Nick Serpone
University of Pavia
437 PUBLICATIONS **18,081** CITATIONS
SEE PROFILE

Spectral Dependence and Wavelength Selectivity in Heterogeneous Photocatalysis. I. Experimental Evidence from the Photocatalyzed Transformation of Phenols

A. Emeline,[†,‡] A. Salinaro,[†] and N. Serpone*[,†]

Department of Chemistry and Biochemistry, Concordia University, 1455 deMaisonneuve Blvd. West, Montreal (Quebec), Canada H3G 1M8 and Department of General Physics II, State University of St. Petersburg, Ulyanovskaya 1, St. Petersburg, Russia 198904

Received: May 24, 2000; In Final Form: September 19, 2000

The photocatalyzed transformation of phenol (PhOH) and 4-chlorophenol (ClPhOH) in air-equilibrated TiO_2 dispersions has been used to examine the spectral behavior of the quantum yields Φ (and photonic efficiencies, η) of loss of these two substrates at various wavelengths. Contrary to the band model of semiconductors and conventional wisdom which predict rapid thermalization of photogenerated charge carriers to the lowest energy levels in their respective conduction and valence band states, and consequently to spectrally independent quantum yields, experimental results demonstrate that in fact the quantum yields of loss of PhOH and ClPhOH are spectrally dependent, displaying well resolved band structures at 3.13, 3.21, 3.32, 3.60, 3.81, 4.28 and 4.57 eV for phenol and at 3.16, 3.25, 3.41, 3.59, 3.70 and 4.15 eV for 4-chlorophenol. These energies correlate with absorption and emission band energies of direct and indirect band-to-band transitions reported earlier by Serpone et al. (*J. Phys. Chem.*, **1995**, *99*, 16655) and with theoretical estimates by Daude and co-workers (*Phys. Rev. B*, **1977**, *15*, 3229) for TiO_2 crystals. Both the spectral dependence of Φ and η and the wavelength selectivity of TiO_2 (S_e and S_h) are discussed in terms of theoretical predictions based on the solution of the continuity equation. The implicit emphasis of this study is the need to rethink the predictions based on the conventional band model of semiconductors. Thermalization of hot carriers may not (in some cases) be as rapid as once envisaged.

Introduction

The past three decades have witnessed much attention on studies of photostimulated processes in heterogeneous (gas−solid, liquid−solid) systems by the photochemical community.[1−10] The extensive studies carried out in numerous laboratories have produced a massive array of experimental data on the photochemical behavior of different heterogeneous systems and in most cases have established the major mechanistic features of photochemical and photophysical processes taking place at solid/gas and solid/solution interfaces. Nonetheless, the quantitative description and characterization of the photostimulated processes in such heterogeneous systems is still a matter of current interest.[11−13] In particular, a major issue has been the lack of an appropriate protocol with which to compare the activities of different photocatalysts in different heterogeneous systems.

A few parameters have been suggested for the characterization of photocatalytic activities in heterogeneous systems. One is the photonic efficiency (η, eq 1) which has been defined as the ratio between the number of molecules formed or degraded in the system per unit time, dN_r/dt (molecules s^{-1}), and the number of photons acting on the system per unit time, $dN_{h\nu(inc)}/dt$ (photons s^{-1}), at a given wavelength (some workers have referred to this, albeit incorrectly, as a quantum yield). In other words, photonic efficiency is a reaction rate normalized to the photon flow from the light source that describes how many molecules are transformed per photon acting on the system.

$$\eta = \frac{\dfrac{dN_r}{dt}}{\dfrac{dN_{h\nu(inc)}}{dt}} \quad (1)$$

Another parameter used to characterize the photochemical activity of heterogeneous systems is the more fundamental quantum yield (Φ) of the photoreaction given by eq 2

$$\Phi = \frac{\dfrac{dN_r}{dt}}{A\left(\dfrac{dN_{h\nu(inc)}}{dt}\right)} = \frac{\dfrac{dN_r}{dt}}{\dfrac{dN_{h\nu(abs)}}{dt}} \quad (2)$$

and defined as the ratio between the number of molecules formed or degraded in the system per unit time, dN_r/dt (molecules s^{-1}), and the number of photons absorbed by the system per unit time, $dN_{h\nu(abs)}/dt$ (photons s^{-1}), at a given wavelength; A represents the fraction of the photon flow absorbed by the heterogeneous system. Thus, the quantum yield represents how many molecules are transformed per absorbed photon. The essential difference between photonic efficiency η and quantum yield Φ is that not every incident photon will necessarily act upon the heterogeneous system and initiate the chemical transformation. Only those photons that are absorbed will do so. Consequently, and especially for weak absorption of light, although the photonic efficiency may be close to 0, the quantum yield may nevertheless reach high values. Appropriate determination of the fraction of absorbed light in heterogeneous systems has made the measurements of quantum yields a complex issue. This problem was solved in solid/gas heterogeneous systems by using either diffuse reflectance

† Concordia University.
‡ State University of St. Petersburg.
* Address all correspondence to this author at Concordia University. FAX: (514) 848−2868 E-mail: serpone@vax2.concordia.ca

10.1021/jp001927o CCC: $19.00
Published on Web 11/02/2000

spectroscopy with a standard reference sample, or a blackbody-like reactor.[14−17] A protocol for determining the fraction of absorbed light in solid/liquid heterogeneous systems has been suggested recently using an integrating sphere assembly.[18,19] With this method, the quantum yield of photobleaching methylene blue and the photodegradation of phenol were determined to be $\Phi = 0.040 \pm 0.003$ in the spectral range 300−400 nm[18] and $\Phi = 0.14 \pm 0.02$ at $\lambda = 365$ nm, respectively.[19]

To establish both the photonic efficiency and the quantum yield of a photostimulated reaction in heterogeneous systems, two important conditions must be satisfied:[20,21] (i) the reaction rate must be linearly dependent on photon flow, and (ii) the reaction rate must be independent of the concentration of reagent. Otherwise, if both photonic efficiency and quantum yield depended on photon flow and reagent concentration, photocatalytic activities as might be described by η or Φ from different heterogeneous systems and different laboratories could not be compared.

In earlier studies[12,19] a simple parameter, the relative photonic efficiency (η_{rel}), was introduced so as to compare photochemical activities of different heterogeneous systems (eq 3).

$$\eta_{rel} = \frac{\eta'}{\eta_{st}} \tag{3}$$

It was described as the ratio between the photonic efficiency of a given reaction (η') to the photonic efficiency η_{st} of a standard reaction (i.e., the photodegradation of phenol over TiO_2 "Degussa P-25" chosen as a standard photocatalyst[12,19]). In turn, this equals the ratio of the corresponding reaction rates under otherwise identical irradiation conditions (eq 4).

$$\eta_{rel} = \frac{\dfrac{dN'_r}{dt}}{\dfrac{dN_{r,st}}{dt}} \tag{4}$$

For comparing photocatalytic activities for the same photocatalyst but for reactions of different reagents under identical irradiation and light absorption conditions, the relative photonic efficiency may also be defined as the ratio of the appropriate quantum yields of the corresponding processes (eq 5).

$$\eta_{rel} = \frac{\Phi'}{\Phi_{st}} \tag{5}$$

Using this approach and the value of the quantum yield of phenol photodegradation over TiO_2 P-25 as the standard reaction and photocatalyst has led to the estimation of the quantum yields of photodegradation of different aromatic compounds.[22]

In many cases, however, both the photonic efficiencies and the so-called quantum yields were determined using broadband radiation rather than under monochromatic irradiation conditions, as required by the definitions of both parameters.[23] This problem would not be an issue if both parameters were spectrally independent. However, for all the solid/gas heterogeneous systems examined earlier,[14−17,24−27] both photonic efficiencies and quantum yields were seen to be spectrally dependent. The spectral dependence of η and Φ may be a rather general phenomenon, and one may therefore expect to observe such dependencies even for solid/liquid heterogeneous systems.

To interpret the spectral dependency of the quantum yield, we recently proposed a model based on the one-dimensional solution to the continuity equation[28] considering the spacial nonuniform photogeneration of charge carriers (electrons and holes) and the diffusion limitation for carriers generated in the bulk of the solid to reach the surface in order to take part in surface chemical reactions. The model predicted that the quantum yield will increase with an increase of the absorption coefficient and that Φ becomes spectrally independent under strong absorption conditions. Another consequence of the solution to the continuity equation was a demonstration that photocatalysts may be spectrally selective; that is, the selectivity of the photocatalyst changes on varying the wavelength of the incident light.[28] This phenomenon was first observed experimentally in solid/gas heterogeneous systems by Kuzmin et al.[29] and by Ryabchuk and co-workers.[30]

The present study examines two cases, namely the photodegradation of phenol and 4-chlorophenol in aqueous TiO_2 dispersions to assess whether the expected quantum yields for the photodegradation of these two substrates are spectrally dependent and whether the photocatalyzed reactions display wavelength selectivity.

Experimental Section

Materials. The photocatalyst was P25 TiO_2 kindly provided by Degussa Canada Ltd. The phenol and 4-chlorophenol were Aldrich reagents and were used as received. Solvents for liquid chromatography were Omnisolv HPLC grade, and the water was doubly distilled.

Procedures. Photonic efficiencies and quantum yields were determined using recently reported protocols.[11,12] The photon flow (ρ) from the irradiation source was established using Aberchrome 540 and ferrioxalate actinometry using well-established standard procedures (see, e.g., ref 23).

All experiments were carried out at pH ~3 (HCl). Typically, irradiation of a phenol solution in an air-equilibrated dispersion with a TiO_2 loading of 0.3 g L^{-1} was carried out in a sphere-like Pyrex reactor using an Oriel 1000-Watt Hg/Xe lamp as the light source whose radiation was filtered through a water filter to remove IR radiation. Appropriate wavelengths of illumination were selected using a monochromator (spectral resolution ca. ± 5 nm). Nonselective "gray" metal supported Pyrex filters were used to attenuate the photon flow, where needed. Rates of the photocatalyzed degradation of phenol and 4-chlorophenol were determined by monitoring the time evolutions of the concentrations of the aromatic compounds during irradiation utilizing liquid chromatographic methods with a Waters HPLC chromatograph (501 pump and either a Waters μBondapak C18 column or a Whatman Partisil 10 ODS-3 column) interfaced to a Shimadzu flow cell for absorption recording. The Shimadzu UV-265 spectrophotometer was also interfaced to an IBM PC computer for data acquisition and handling. For the determination of the quantum yields the initial concentrations used were 0.23 mM for phenol and 0.20 mM for 4-chlorophenol chosen after experiments as displayed in Figure 1. The fraction of light scattered and absorbed by theTiO_2 catalyst was assessed with the UV-265 spectrophotometer equipped with an integrating sphere using a method developed earlier.[12,19] Recording parameter settings, data collection, and data processing were carried out using the Spectroscopy Interface Software, Version 3 (Shimadzu Scientific Instruments, Inc.).

Results

Two essential conditions must be satisfied to determine photonic efficiencies and unique quantum yields of surface photochemical reactions in heterogeneous media:[31] (i) reaction rates must be independent of the concentration of reagents, that

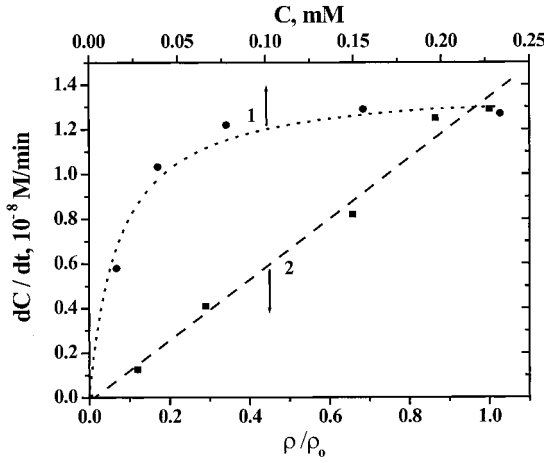

Figure 1. Dependencies of the rate of photodegradation of phenol over TiO_2 on (1) the phenol concentration, and on (2) photon flow at photoexcitation with light at $h\nu = 3.38$ eV (365 nm).

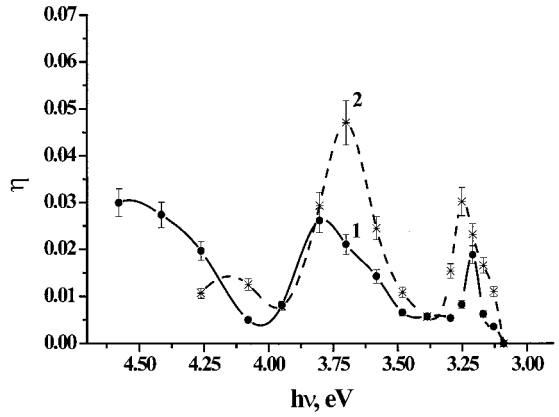

Figure 2. Spectral dependencies of the photonic efficiencies of the photodegradation of (1) phenol and (2) 4-chlorophenol.

is, quantum yields must be determined under conditions of zero-order kinetics; and (ii) the rates must scale linearly with the intensity (or photon flow) of the incident *actinic* light. To verify whether these conditions were satisfied in the present cases, we carried out a set of control experiments to measure reaction rate dependencies on the concentration of phenol and on the light intensity at three different wavelengths (380, 365, and 334 nm). The results showed that under the chosen experimental conditions the initial reaction rates for the degradation of the two test substrates reached saturation with respect to concentration and were linearly dependent on light intensity (see, e.g., Figure 1). Consequently, the photonic efficiencies and the quantum yields measured under these conditions are uniquely defined, are maximal and depend only on the intrinsic properties of the photocatalyst, so that any wavelength dependencies of the photonic efficiencies and quantum yields reflect the features of photoexcitation and of transfer of the charge carriers from the catalyst particle bulk to the surface and then to the reagent molecules, features that are appropriate to the TiO_2 specimen used.

The experimental spectral dependencies of the photonic efficiency for the photocatalyzed degradation of phenol and chlorophenol are presented in Figure 2 and summarized in Table 1. The estimated positions of the maxima (and shoulders) of the spectral dependencies are summarized in Table 2.

We have noted earlier that the quantum yield differs from the photonic efficiency because the former takes into account the number of photons actually absorbed by the system per unit time, rather than the number of photons incident on such system. Quantum yields were estimated with the aid of the spectral distribution of the fraction of light absorbed obtained for the TiO_2 (Degussa P25) loading employed in a previous study.[12] Figure 3 illustrates the spectral dependencies of the quantum yield of the photocatalyzed degradation of phenol and chlorophenol over TiO_2; the experimental quantum yields at various excitation energies are collected in Table 1. The dependencies display well resolved band structures with two principal band maxima at ca. 3.2 and 3.7 eV together with some additional finer details (see Table 2). These correspond to the energies of indirect and direct band-to-band transitions in the anatase polymorph (see below and Table 2).

TABLE 1: Experimental Quantum Yields, Photonic Efficiencies, and Relative Photonic Efficiencies for the Photodegradation of Phenol ($C_o = 0.23$ MM) and 4-chlorophenol ($C_o = 0.20$ MM) over TiO_2 (Degussa P25) Aqueous Dispersions Illuminated at Various Wavelengths

λ_{excit}, nm	$h\nu_{excit}$ eV	η_{PhOH}[a]	Φ_{PhOH}[a]	η_{ClPhOH}[a]	Φ_{ClPhOH}[a]	η_{rel}
270	4.58	0.03	0.062			
280	4.41	0.027	0.054			
290	4.26	0.02	0.04	0.011	0.021	0.54
303	4.07	0.0051	0.011	0.012	0.026	2.48
313	3.95	0.0082	0.019	0.0079	0.018	0.97
325	3.8	0.026	0.073	0.029	0.082	1.1
334	3.7	0.021	0.075	0.047	0.17	2.2
345	3.58	0.014	0.076	0.024	0.13	1.7
355	3.48	0.0066	0.048	0.011	0.078	1.6
365	3.39	0.0057	0.053	0.0057	0.052	0.99
375	3.3	0.0054	0.061	0.015	0.17	2.8
380	3.25	0.0082	0.11	0.03	0.4	3.7
385	3.21	0.019	0.26	0.023	0.32	1.2
390	3.17	0.0063	0.097	0.016	0.26	2.6
395	3.13	0.0036	0.057	0.011	0.18	3.1
400	3.09	0	0	0	0	-

[a] Estimated error ca. ±10%.

The spectral dependence of the ratio of the quantum yields of 4-chlorophenol photodegradation to the quantum yield of phenol photodegradation (i.e., the relative photonic efficiency for the photodegradation of chlorophenol, see Introduction) is presented in Figure 4.

All three parameters (namely, quantum yield, photonic efficiency, and relative photonic efficiency) described earlier, which can be used to characterize the photoactivity of the TiO_2 photocatalyst with regard to phenol and chlorophenol photodegradation, show spectrally dependent behavior. Spectral maxima and shoulders of all parameters are also summarized in Table 2.

The kinetics of formation of benzoquinone (one of the principal intermediates) were determined on photoexcitation of 4-chlorophenol at several wavelengths of the incident light. Note the striking differences in the kinetic behavior in the formation of benzoquinone at the four wavelengths illustrated (Figure 5). Relevant quantum yields for the initial formation of this intermediate are summarized in Table 3.

Discussion

Spectral Dependence of Quantum Yields. For a titania/phenol aqueous heterogeneous system and within the spectral range 280−400 nm, light absorption concerns mostly TiO_2 because the two organic substrates examined do not absorb in this wavelength range under the conditions used. A result of this primary photoexcitation of the photocatalyst is generation of electron/hole pairs (eq 6).

$$TiO_2 + h\nu \rightarrow e^- + h^+ \qquad (6)$$

Those charge carriers that reach the photocatalyst surface are

TABLE 2: Estimated Energy Maxima for the Photonic Efficiencies and Quantum Yields of the Photodegradation of Phenol and 4-Chlorophenol, and Comparison with Theoretical Estimates and Experimental Energies (from absorption and photoluminescence) of Indirect and Direct Electronic Transitions

$h\nu$ (theor)[a] eV	$h\nu$ (Abs/Lum)[b] eV	band maxima eV	Φ_{PhOH} (calcd)[c]	band maxima eV	Φ_{ClPhOH} (calcd)[c]
3.05	2.97	3.13	0.05	3.16	0.23
3.19	3.21	3.21	0.23	3.25	0.39
3.45	3.61−3.68	3.32	0.06	3.42	0.051
3.59	3.61−3.68	3.6	0.072	3.62	0.096
4.05	4.03−4.04	3.8	0.065	3.72	0.093
4.3		4.28	0.023	4.14	0.029
		4.57	0.059		

[a] From ref 32. [b] From ref 45. [c] Obtained following a deconvolution of the spectral envelopes of Figures 2 and 3 using the PeakFit software version 4.

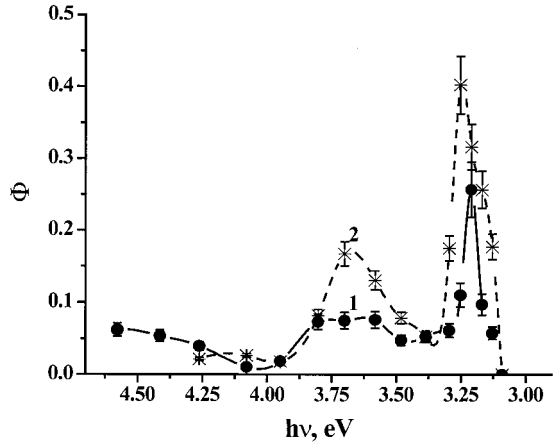

Figure 3. Spectral dependencies of the quantum yields of the photodegradation of (1) phenol and (2) 4-chlorophenol.

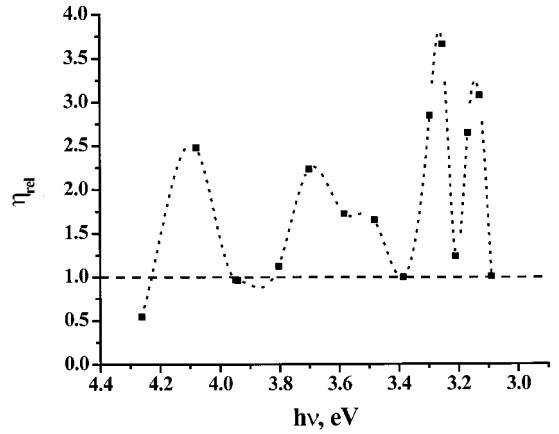

Figure 4. Spectral dependence of the relative photonic efficiency of photodegradation of 4-chlorophenol with respect to the photodegradation of phenol.

poised to participate in surface chemical processes. Thus, regardless of the mechanism of the photocatalytic process, its rate will depend on the surface concentration of the corresponding charge carriers, n_s. In the steady-state approximation, the latter is determined (a) by the rate of photostimulated carrier generation in the bulk of the photocatalyst, (b) by the rate of carrier diffusion flow from the bulk to the surface, and (c) by their decay through surface recombination and reaction pathways. For the one-dimensional model the surface concentration of the carriers is expressed[28] by eq 7

$$n_s = \frac{2(1 - e^{-\alpha d})\,\chi\rho\alpha L^2}{D\left(\tanh\left(\frac{d}{2L}\right) + \xi\right)(1 - \alpha^2 L^2)}\left[\tanh\left(\frac{d}{2L}\right)\coth\left(\frac{\alpha d}{2}\right) - \alpha L\right] \quad (7)$$

where D is the diffusion coefficient of the carriers, χ is the quantum yield of internal photoeffects (generation of carriers), ρ is the photon flow of the incident light, α is the absorption coefficient of the photocatalyst at a given wavelength, $L = (D\tau)^{1/2}$ is the diffusion length of the carriers (τ is the lifetime of carriers in the bulk), and $\xi = s\,L/D$ is taken as the ratio of surface recombination (s) to bulk recombination rates. Then, for the simplified primary step (eq 8) involving reagent molecules M interacting with surface carriers of the proper sign, the photonic efficiency η of the disappearance of M molecules is given by eq 9, and the quantum yield Φ of the primary reaction (eqn. 8) is described by eq 10.

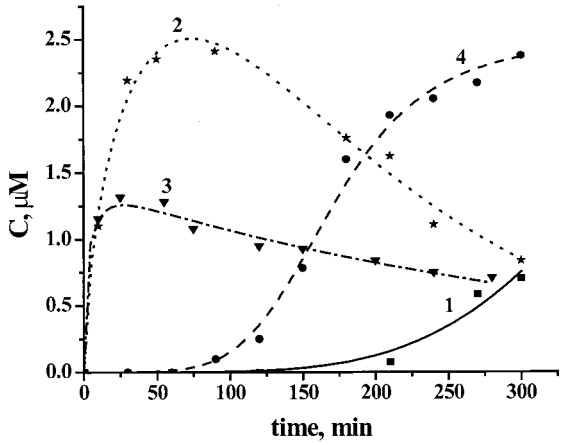

Figure 5. Kinetics of formation of benzoquinone during the photocatalyzed transformation of 4-chlorophenol (C_o = 0.20 mM) at photoexcitation with light at (1) $h\nu$ = 3.21 eV (385 nm); $\rho = 2.08 \times 10^{15}$ photons s^{-1}; (2) $h\nu$ = 3.38 eV (365 nm) $\rho = 2.26 \times 10^{16}$ photons s^{-1}; (3) $h\nu$ = 3.53 eV (350 nm) $\rho = 4.4 \times 10^{15}$ photons s^{-1}; and (4) $h\nu$ = 3.70 eV (334 nm) $\rho = 3.9 \times 10^{15}$ photons s^{-1}.

TABLE 3: Experimental Initial Quantum Yields and Selectivities in the Formation of Benzoquinone during the Photodegradation of 4-Chlorophenol (C_o = 0.20 mM) over TiO_2 (Degussa P25; Loading 0.3 g L^{-1}) in Aqueous Dispersions Illuminated at Various Wavelengths

Run[a]	$h\nu$, eV (λ, nm)	ρ (photons s^{-1})	Φ_{BQ}[b]	S_{BQ}[b]
1	3.21 (385)	2.08×10^{15}	0.0024	0.008
2	3.38 (365)	2.26×10^{16}	0.03	0.58
3	3.53 (350)	4.4×10^{15}	0.086	0.78
4	3.70 (334)	3.9×10^{15}	0.001	0.006

[a] Numbers correspond to the curves in Figure 5. [b] Estimated error ca. ±15%.

$$M + h^+ (e^-) \rightarrow M^+ (M^-)\ (k_r) \quad (8)$$

$$\eta = \frac{k_r\, M\, 2(1 - e^{-\alpha d})\chi\alpha L^2}{D\left(\tanh\left(\frac{d}{2L}\right) + \xi\right)(1 - \alpha^2 L^2)}\left[\tanh\left(\frac{d}{2L}\right)\coth\left(\frac{\alpha d}{2}\right) - \alpha L\right] \quad (9)$$

$$\Phi = \frac{k_r M \chi \alpha L^2}{D\left(\tanh\left(\frac{d}{2L}\right) + \xi\right)(1 - \alpha^2 L^2)}\left[\tanh\left(\frac{d}{2L}\right)\coth\left(\frac{\alpha d}{2}\right) - \alpha L\right] \quad (10)$$

As soon as free charge carriers are photogenerated in a few femtoseconds (i.e., 10^{-15} s), two possibilities may arise. The first is that if there exists rapid communication between different subband states in the valence and conduction bands, in a few picoseconds ($\sim 10^{-10}$ s) the photocarriers will occupy the lowest states in their corresponding bands (i.e., they become thermalized). At moderate excitation energies, their distributions obey (quasi-)Boltzmann statistics with the carrier temperature equal to ambient temperature, and the carriers will have similar average mobilities and lifetimes and become indistinguishable, regardless of the initial state occupied immediately upon photoexcitation. In terms of time scale, this means that the time of energy relaxation of the carriers τ_{rlxn} is much shorter than their lifetimes $\tau_{e,h}$; that is, $\tau_{rlxn} \ll \tau_{e,h}$. In such instance, the diffusion coefficient D and diffusion length L, as well as the recombination parameters in eqs 8−10, are constant, and all the spectral variations of either the photonic efficiency η or the quantum yield Φ would have their origins simply from variations in the absorption coefficient α in the product αL and αd. For example, the quantum yield of the surface photoreaction (eq 8) within a single absorption band increases with an increase of α and becomes spectrally independent when $\alpha L \gg 1$, provided that the diffusion length L of the carriers is much less than the crystal size, i.e., for $L \ll d$.[28] Thus, one may expect to observe a spectral dependence of the quantum yield and photonic efficiency just at the edge of the intrinsic absorption where the absorption coefficient rises from $\sim 10^2$ to about 10^4-10^6 cm^{-1}. Where the absorption coefficient is of the same order of magnitude as the diffusion length, weak spectral fluctuations of the quantum yield (and photonic efficiency) may be expected.

A second possibility appears when the energy relaxation time is longer than the lifetime of the free carriers; i.e., when $\tau_{rlxn} \gg \tau_{e,h}$. This possibility arises when elastic collisions dominate the inelastic collisions as a major pathway for electron/phonon interactions in the solid. This pathway leads to a fast momentum relaxation and to the establishment of equilibrium in the momentum in the electronic subsystem during a time when energy relaxation is not yet completed. In particular, this may lead to a higher population of the valleys of the subbands of higher energy compared to the thermally equilibrated state (Figure 6),[32] and thus to a higher temperature of electron gas because of the presence of hot carriers.[33,34]

An additional cause for the longer energy relaxation times arises if communication between the different states in the respective conduction and valence bands in nanoparticles is much less effective than in bulk solid crystals or if there exists no communication between such states. The reason for weak (or nonexistent) communication between such states in nanoparticles, unlike bulk crystals, could be that the translation symmetry in spatially confined nanoparticles is valid only for the short-length crystal units, and that the number of atomic states forming the band states is very limited compared to the number of atomic states in bulk crystals. In the simplest of cases, the number of states (Q) scales with the ratio of the crystal volume (V) to the volume of the elementary unit (V_o); that is,

$$Q \cong \frac{V}{V_o} \quad (11)$$

Consequently, if the number of states for the bulk crystal is very large because of a larger number of elementary units that form the crystal, the number of such states in nanosized particles is likely to be somewhat limited. A similar effect arises as a quantization in the depletion layer at the surface of bulk semiconductors when a thinner layer (with respect to the effective mass of carriers) causes formation of localized weakly or noncommunicating electronic states in spatially confined depletion layer (note, that nanoparticles are also spatially confined system).[35−38]

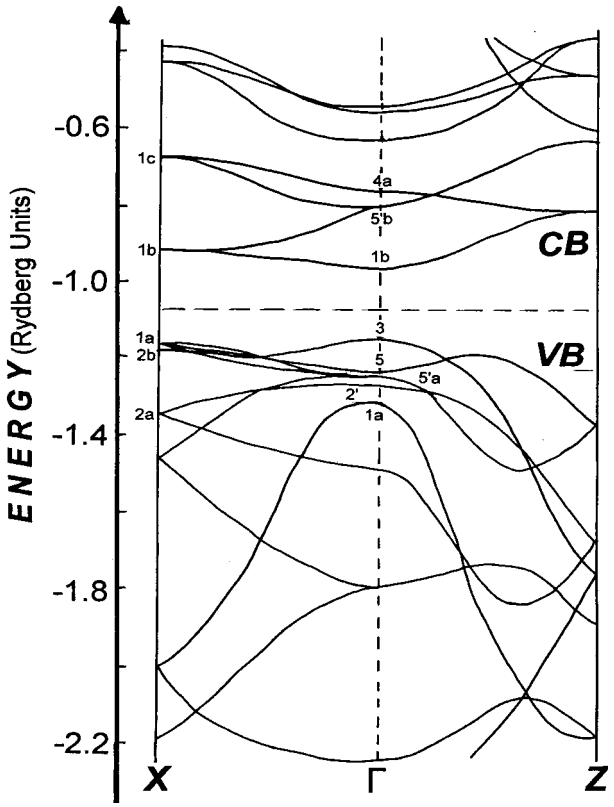

Figure 6. Graph illustrating some relevant valence and conduction band levels in the Brillouin zone for a TiO_2 crystal in the ***X*** and ***Z*** edges and in the center Γ. Adapted from ref 32.

Taking the average size of the particle as ca. 30 nm (typical of Degussa P25 TiO_2), the volume of the particle $V \approx 2.7 \times 10^{-27}$ m^3, and the volume of the elementary unit of anatase $V_o \approx 10^{-30}$ m^3. The number of electronic states in the bands is then ca. 10^6, whereas in the bulk crystal $Q \gg 10^6$. Accordingly, energy relaxation in nanoparticles may be more difficult. In turn, the carriers occupying the different valleys of the different states in the conduction and valence bands (Figure 6) will be characterized by different lifetimes and different mobilities (and diffusion coefficients), and consequently different diffusion lengths. Hence, the lifetimes, the mobilities and the diffusion lengths in eqs 8−10 become spectrally dependent because the population of the given electronic states depends on the energy of the photons. Consequently, the surface concentration of carriers becomes spectrally dependent because of the spectral variation of carrier mobilities.

An appropriate description of the spectral dependence necessitates that we take into account (a) the size of the TiO_2 particles which for the Degussa P25 specimen is ca. 20−40 nm,[39] (b) the spectral variation of the absorption coefficient ($\alpha \approx 10^2$ to 10^6 cm^{-1}), and (c) the diffusion length for electrons ($L_e \approx 10^{-6}$ cm). The diffusion coefficient for Degussa P25 titania is taken to be $D = 5 \times 10^{-3}$ cm^2 s^{-1}, [40,41] and the lifetime of free electrons τ_e is a few tens of picoseconds.[42,43] The diffusion length of free holes (L_h) is taken to be longer than the diffusion

length of electrons (i.e., $L_e \ll L_h$) since the lifetime of electrons and holes are of about the same magnitude, but hole mobility appears to be faster than for electrons.[40] This assumption is in keeping with the rather broad valence band of TiO_2.[32,44] Note that a precise estimate of the diffusion length of free holes is difficult because of the lack of appropriate experimental data. The rate of surface recombination (s) for a highly defective surface of nanoparticles is likely to be around 10^5 cm s^{-1}. Then the variation of α from 10^2 to ca. 10^5 cm^{-1} at the fundamental absorption edge, which is associated with indirect transitions, corresponds to the theoretical case of weak light absorption when αL and αd are much less than unity. Also note that even a maximal absorption coefficient of 10^6 cm^{-1} at the higher photon excitation energies, corresponding to direct band-to-band transitions, will not satisfy the conditions of strong light absorption considered previously because they would require that $\alpha L \gg 1$ and that $\alpha d \gg 1$.[28]

Earlier theoretical considerations and experimental evidence[15,17,28] have inferred for the case of weak light absorption (i) that the quantum yield Φ is spectrally independent (i.e., $\Phi \neq fn(\alpha)$, eq 12), (ii) that the photonic efficiency η follows the absorption spectrum (i.e., $\eta = fn(\alpha)$; eq 13) either within a single absorption band, or in a complex absorption band if the carriers are formed as a result of light absorption in the band and occupy the same states (corresponding to a thermally equilibrated system) in their respective conduction and valence bands, and (iii) that the quantum yield of carrier formation χ is spectrally independent.

$$\Phi = \frac{2\, k_{tr} S_o \chi L^2}{Dd}\left[\frac{\tanh\left(\frac{d}{2L}\right)}{\tanh\left(\frac{d}{2L}\right)+\xi}\right] \qquad (12)$$

$$\eta = \frac{2\, k_{tr} S_o \chi L^2 \alpha}{D}\left[\frac{\tanh\left(\frac{d}{2L}\right)}{\tanh\left(\frac{d}{2L}\right)+\xi}\right] \qquad (13)$$

By contrast, in the case of the photocatalyzed degradation of phenol and 4-chlorophenol over TiO_2 particles, the spectral distributions of the corresponding photonic efficiencies (Figure 2) and the quantum yields (Figure 3) demonstrate a well resolved band structure. In our previous study,[15,28] we described the reasons for observing band-like spectral dependencies of quantum yields of surface photochemical processes for the case of weak extrinsic light absorption by lattice defects. We concluded that the band-like spectral dependence of Φ is caused by an overlap of different absorption bands corresponding to different types of defects that do not communicate with each other and that differ by the quantum yield of internal photoeffects. In particular, the spectral dependence was observed where active and inactive absorption bands overlapped.[15,28]

The fundamental absorption spectrum of TiO_2 particles is formed by several direct and indirect electronic band-to-band transitions.[32] A review of experimental[45−47] and theoretical[32,44,48] data indicates that the edge of intrinsic absorption by TiO_2 is formed by indirect transitions from the edge to the center of the Brillouin zone (BZ), for example $X_{1a} \rightarrow \Gamma_{1b}$ and $X_{2b} \rightarrow \Gamma_{1b}$, as well as by indirect transitions from the center to the edge, i.e., $\Gamma_3 \rightarrow \boldsymbol{X}_{1b}$ (Figure 7). The lowest energy direct transition $\Gamma_3 \rightarrow \Gamma_5$ is forbidden.[32] The first allowed direct transitions occur at the $\boldsymbol{X}$ edge of the Brillouin Zone: namely, $\boldsymbol{X}_{1a} \rightarrow \boldsymbol{X}_{1b}$ (3.45 eV) and $\boldsymbol{X}_{2b} \rightarrow \boldsymbol{X}_{1b}$ (3.59 eV), and the next allowed lowest energy transitions are $\Gamma_{5'b} \rightarrow \Gamma_{1b}$ (4.05 eV) and $\Gamma_{2'} \rightarrow \Gamma_{1b}$ (4.3 eV). Thus, as a result of band-to-band electronic transitions during photoexcitation with different photon energies, electrons initially occupy different conduction band states, whereas holes of various energies occupy different valence band states.

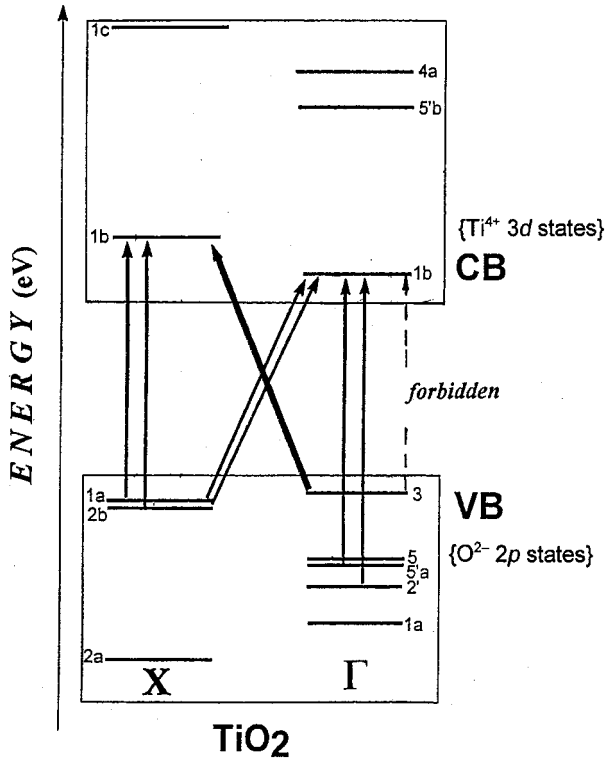

Figure 7. Energy level diagram summarizing the relevant allowed direct and allowed but phonon-assisted indirect electronic transitions between valence and conduction band states in TiO_2. Adapted from ref 32. (The numbers refer to the labels of the states as in Figure 6).

Despite the notion that the fundamental absorption band of TiO_2 is formed by an overlap of different electronic transitions (see above), the concept of inactive absorption or absorption with different quantum yields of internal photoeffects cannot be applied to the case of intrinsic light absorption because each absorbed photon causes generation of electron−hole pairs with a quantum yield of 1, and no inactive background absorption exists. Thus, the only reason for observing a spectral dependence at the edge of the intrinsic absorption band is that the photogenerated carriers in the different states have different recombination constants (i.e., different recombination cross-sections), and consequently different lifetimes, different mobilities, and different rate constants for the surface reactions.[28] Because of weak communication between the different states, the carriers do not thermalize rapidly, and they maintain the corresponding parameters attributed to the given state during their lifetime in that state. This means that in eqs 8−10 and eqs 12 and 13 either that the parameters D, L, and ξ are spectrally dependent or that the concept of overlapping different absorption bands is applicable, which correspond to different band-to-band transitions and which lead to different energy distributions of carriers in the bands and to different efficiencies of photoprocesses for each transition. In this case, however, it is the different lifetimes of carriers and their mobilities, as well as their different ability to be localized at the surface and their reactivity that are responsible for the different efficiencies of photoexcitation of the solid in the fundamental absorption band, instead of differences in the quantum yields of internal photoeffects for weak extrinsic light absorption. Hence, the spectral dependence of the quantum yield and of the photonic efficiency

SCHEME 1

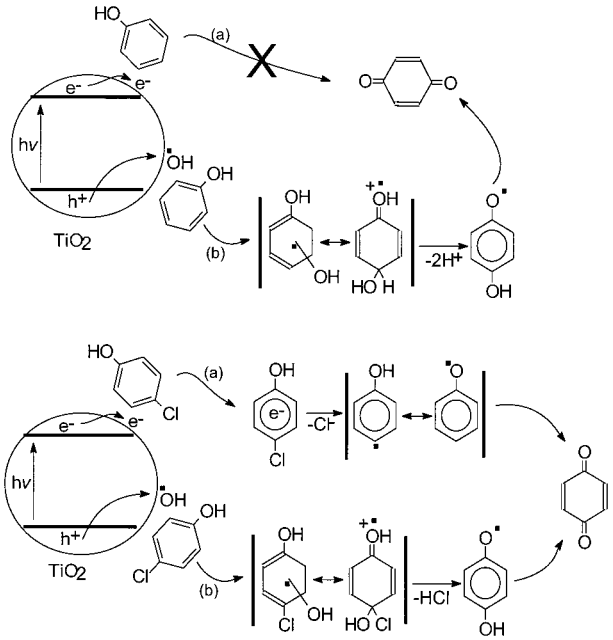

can be estimated from eqs 12 and 13, respectively, by applying the spectral variation of the average diffusion length and carrier lifetimes, or by considering both of these two parameters as being constant within each of the single absorption band corresponding to a given band-to-band transition.

Experimentally, the total quantum yield is obtained from eq 14 and the photonic efficiency from eq 15

$$\Phi_{\text{total}} = \frac{\sum_i A_i \Phi_i}{\sum_i A_i} \tag{14}$$

$$\eta_{\text{total}} = \sum_i \eta_i \tag{15}$$

where A_i is the fraction of photons absorbed for a given transition, Φ_i is the quantum yield within a single absorption band for a given transition (eqs 10 and 12), and η_i is the photonic efficiency also within a single absorption band corresponding to a given transition (eqs 9 and 13).

The first step in the photocatalyzed degradation of phenol (see Scheme 1) is the interaction of phenol molecules with surface trapped holes, more precisely with surface-trapped •OH radicals formed by trapping of holes by surface OH^-_{surf} groups (eqn 16).

$$h^+ + OH^-_{surf} \rightarrow {}^{\bullet}OH_{surf} \tag{16}$$

At the fundamental absorption edge, holes are formed in the $\boldsymbol{X}_1$, $\boldsymbol{X}_2$, and Γ_3 states due to indirect transitions (2.91, 3.05, and 3.19 eV, respectively), which of necessity are phonon-assisted. Consequently, holes at the edge of the BZ are heavier than those generated at the center of BZ, and communication between these states during the carrier lifetimes may be somewhat difficult. To the extent that hole mobilities in different states are (expectedly) different causes the band-like spectral dependencies of photonic efficiencies and quantum yields to be observed in the photodegradation of phenol at the edge of the fundamental absorption.

The diffusion length of photogenerated holes should be comparable to the particle size of the photocatalyst, since the quantum yield achieves a rather significant value ($\Phi \sim 0.25$). At higher photoexcitation energies, direct electronic transitions at the $\boldsymbol{X}$-edge of BZ take place leading to the generation of holes in the $\boldsymbol{X}_1$ and $\boldsymbol{X}_2$ states, the same states involved in the indirect transitions at the fundamental absorption edge. In this case, however, the absorption coefficient becomes comparable to the diffusion length and to the crystalline size, and thus the spectral variation of αd and αL in eqs 8−10 also contributes to the observed spectral dependence of the quantum yields. This contribution demonstrates itself within the photon energy range 3.47 eV to 3.95 eV as an increase of the quantum yield until it reaches the nearly constant value between 3.58 and 3.80 eV followed by its decrease beyond this range. An example of such a behavior was previously considered by Emeline and coworkers,[28] who assumed that the increase of the absorption coefficient in the relation αL within the absorption band causes the increase in the quantum yield until $\alpha L \gg 1$, at which point Φ becomes spectrally independent.

The spectral dependencies of the photonic efficiency (Figure 2) and the quantum yield (Figure 3) of the photodegradation of 4-chlorophenol is qualitatively similar to those for phenol photodegradation. We infer from this that the spectral dependencies are caused by the same electronic band-to-band transitions that generate free electrons and holes. However, unlike phenol, the mechanism of photodegradation of 4-chlorophenol may involve interaction of the phenol with both electrons and holes (see Scheme 1),[49] so that the total quantum yield of 4-chlorophenol disappearance is the sum of quantum yields of degradation caused by electrons Φ_e and holes Φ_h

$$\Phi_{\text{ClPhOH}} = \Phi_{\text{e}} + \Phi_{\text{h}} \tag{17}$$

and the total photonic efficiency is the sum of the corresponding photonic efficiencies of photodegradation caused by both electrons η_{e} and holes η_{h}, respectively:

$$\eta_{\text{ClPhOH}} = \eta_{\text{e}} + \eta_{\text{h}} \tag{18}$$

If we further assume that both the quantum yields and photonic efficiencies of 4-chlorophenol photodegradation caused by surface-bound holes are similar to the photonic efficiencies and quantum yields of phenol disappearance also caused by holes (this is true if the kinetics of attack of phenol and 4-chlorophenol by •OH radicals in the heterogeneous media are nearly identical, which is the case in homogeneous media ($k_{\text{OH}} = 9.6 \times 10^9\ \text{M}^{-1}\ \text{s}^{-1}$ for phenol and $k_{\text{OH}} = 9.3 \times 10^9\ \text{M}^{-1}\ \text{s}^{-1}$ for 4-chlorophenol[50,51]), then the relative photonic efficiency η_{rel} will be given by

$$\eta_{\text{rel}} = \frac{\eta_{\text{ClPhOH}}}{\eta_{\text{PhOH}}} = \frac{\Phi_{\text{ClPhOH}}}{\Phi_{\text{PhOH}}} \tag{19a}$$

and

$$\eta_{\text{rel}} = 1 + \frac{\eta_{\text{e}}}{\eta_{\text{h}}} = 1 + \frac{\Phi_{\text{e}}}{\Phi_{\text{h}}} = 1 + \frac{R_{\text{e}}}{R_{\text{h}}} \tag{19b}$$

where R_{e} and R_{h} are the rates of the primary steps in the 4-chlorophenol photodegradation caused by electrons and holes, respectively. Thus, η_{rel} = ca. 1 (horizontal line in Figure 4) if at a given wavelength of photoexcitation the degradation of 4-chlorophenol caused by electrons is negligible relative to oxidation by holes (indeed observed at $h\nu = 3.2$, 3.4, 3.8−3.95 eV, and 4.25 eV), and if the spectral variation in η_{rel} is caused by the spectral variation of the ratio of the corresponding rates R_{e} and R_{h} (quantum yields, photonic efficiencies), which

in turn depend on the spectral changes of the ratio between the surface concentrations of electrons [e_s] and holes [h_s] and the spectral variation of rate constants k_{re} and k_{rh} (eq 20).

$$\eta_{rel} = 1 + \frac{k_{re}[e_s]}{k_{rh}[h_s]} \tag{20}$$

Substituting the corresponding values of the quantum yields or the photonic efficiencies using eqs 12 and 13, respectively, with the corresponding parameters for electrons and holes, we obtain

$$\eta_{rel} = 1 + \frac{k_{re}\,\tau_e}{k_{rh}\,\tau_h}\left(\frac{\tanh\left(\frac{d}{2L_e}\right)\left[\tanh\left(\frac{d}{2L_h}\right) + \xi_h\right]}{\tanh\left(\frac{d}{2L_h}\right)\left[\tanh\left(\frac{d}{2L_e}\right) + \xi_e\right]}\right) \tag{21}$$

Hence, the spectral variation of the relative photonic efficiency depends on the spectral variations of diffusion lengths and lifetimes of carriers owing to different populations of the different valence band states and conduction band states. Note that for small nanosized particles the lifetime of carriers in the bulk, τ, may reflect the time of escape of the carriers from the bulk to the surface (eq 22):

$$\tau = \frac{d^2}{D} = \frac{d^2[e]}{\mu\kappa T} \tag{22}$$

The condition expressed by eq 22 corresponds strictly to the case where $L \gg d$, but formally it is taken to reflect the transformation to the conventional kinetic behavior of carriers. However, for very small particles another behavioral feature caused by spatial confinement may appear and a stochastic approach should then be contemplated.[52,53] The spectral dependence of reaction efficiencies for such small sized particles (i.e., when $d \ll L$) could then be caused by different reactivities of the surface carriers on photoexcitation by photons of different energies, i.e., by a spectral variation of k_{re} and k_{rh}, and by a spectral variation of the recombination constants (either bulk or surface recombination).

Wavelength Selectivity of Photodegradation. The relative photonic efficiency η_{rel}, as defined by eq 20, represents the inverse of the selectivity of the photocatalyst (eq 23), provided that only the two reaction pathways considered in Scheme 1 take place. The selectivity of the photocatalyst with respect to oxidation by holes (S_h) and reduction by electrons (S_e), respectively, is described by eqs 23 and 24.

$$S_h = \frac{R_h}{R_h + R_e} = \frac{k_{rh}[h_s]}{k_{rh}[h_s] + k_{re}[e_s]} = \frac{\frac{k_{rh}[h_s]}{k_{re}[e_s]}}{\frac{k_{rh}[h_s]}{k_{re}[e_s]} + 1} \tag{23}$$

$$S_e = \frac{R_e}{R_h + R_e} = \frac{k_{re}[e_s]}{k_{rh}[h_s] + k_{re}[e_s]} = \frac{\frac{k_{re}[e_s]}{k_{rh}[h_s]}}{\frac{k_{re}[e_s]}{k_{rh}[h_s]} + 1} \tag{24}$$

Clearly, alteration of the [e_s]/[h_s] ratio will change the principal reaction pathway and favor the formation of one or more reaction products and intermediates.[28] Assuming that the rate constants of 4-chlorophenol interaction with surface electrons and •OH radicals are nearly identical (in homogeneous phase, $k_e = 1.5 \times 10^9$ M^{-1} s^{-1} and $k_{OH} = 9.3 \times 10^9$ M^{-1} s^{-1} [49,51]) and considering that on average a single photon acts on the particle about every 10^{-5} s under our experimental conditions, we infer that the limiting steps of the photoreactions are the photogeneration and diffusion of carriers to the surface, and subsequently the surface trapping of carriers to form •OH radicals or electrons centers (such as Ti^{3+}). Thus, the selectivity of a photocatalyst will depend on the spectral variation of the mobilities of carriers which alter the ratio of the surface concentration of carriers and/or active surface centers.

Benzoquinone is one of the intermediates formed in the photodegradation of 4-chlorophenol regardless of the reaction pathway (see Scheme 1). However, in the case where the surface concentration of electrons [e_s] is greater than [h_s] in eq 23, the kinetic behavior will reflect more the sequence (a) than (b), whereas if [e_s] is smaller than [h_s] the major pathway will be oxidation by holes (sequence (b)) and the kinetics should then reflect the concentration evolution of the appropriate intermediate.

The result of these expectations is observation of different kinetic behaviors for the formation of benzoquinone. At those wavelengths where the relative photonic efficiency is about 1 (see horizontal line in Figure 4), and thus the selectivity for oxidation by holes (OH•-radicals) also approaches 1 (compare eqs 23 and 24), the kinetics of formation of benzoquinone correspond to the kinetic behavior often observed for consecutive reactions (eq 25),[54] whereby for one case intermediate B forms rapidly followed by its slow decay, that is $k_B \gg k_C$.

$$A \xrightarrow{k_B} B \xrightarrow{k_C} C \rightarrow\rightarrow \text{products} \tag{25}$$

The •OH-radical initiated reaction sequence goes through a fast radical process(es) to form benzoquinone, a behavior that seems typical for excitation at $h\nu = 3.38$ and 3.53 eV. Note also, that the selectivity of benzoquinone formation is close to unity at these energies (see Table 3). By contrast, for excitation at $h\nu = 3.25$ and 3.70 eV, where the contribution of electrons into the total reaction may be significant, the selectivity of the photocatalyst (eqs 23 and 24) turns toward an electron initiated reaction pathway (sequence (a) of Scheme 1) and the behavior of benzoquinone formation kinetics become different and follow the typical behavior of formation of intermediate C in reaction 25; the selectivity of benzoquinone formation is close to zero at these excitation energies (Table 3). The electron initiated reaction pathway presumably goes through some relatively stable intermediate(s) before production of benzoquinone. Also noteworthy is the difference between the quantum yields of benzoquinone formation at photons energies $h\nu = 3.38$ and 3.53 eV when the reaction with trapped holes is the dominating process, and for excitation at $h\nu = 3.25$ and 3.70 eV when the reductive pathway becomes more significant (Table 3). Thus, the different kinetic behavior of benzoquinone formation can be rationalized in terms of the spectral selectivity of photocatalysts.[28]

This behavior also accords with the spectral variations of the quantum yields of phenol and 4-chlorophenol photodegradation and with the relative photonic efficiency of 4-chlorophenol destruction. These infer that the spectral variation of carrier mobilities (hence, diffusion length) is connected to the different population of the separate electronic states in the valence and conduction bands. The population changes parallel the changes in the surface concentration of carriers and in their ratio [e_s]/[h_s] to alter both the activity and selectivity of the photocatalyst. Note that the spectral difference in population of the electronic states of a photocatalyst can also lead to the spectral variation

of the corresponding reaction rate constants, and hence also affect the selectivity of the photocatalyst.

Concluding Remarks

The photocatalyzed degradation of phenol and 4-chlorophenol was reexamined to assess the spectral dependence of process photonic efficiencies and quantum yields; these were determined using a protocol reported earlier.[11,12] In both cases, the reactions displayed a well-defined spectral dependence with some fine structure. The results contrast with expectations based on the classical band model of semiconductors (and on conventional wisdom), which would predict that the photogenerated charge carriers would thermalize very rapidly and any reaction would simply result from these thermalized carriers; that is, there should be no spectral dependence. By contrast, a model based on the solution to the continuity equation for a one-dimensional crystal proposed previously[28] predicted not only a spectral dependence for the quantum yields but also suggested a selectivity for the photocatalyst. The experimental results clearly point to the need for a reconsideration of the band model to take into account the existence of conduction band states and valence band states that may not communicate effectively with each other within their respective bands. Lack of this communication bears on the various factors that affect the properties of charge carriers, and consequently on the photocatalytic process. One important conclusion from this study is that thermalization of carriers may not be as fast as conventional wisdom might dictate. For the 4-chlorophenol, we have also inferred that at certain wavelengths of excitation a noninsignificant electron initiated reduction takes place which also contributes to the overall quantum yield of the degradation of this chlorinated phenol. Subsequent work will address this wavelength selectivity using substrates that yield well-defined intermediates and products when both photooxidative and photoreductive degradations may occur concomitantly.[55]

Acknowledgment. Support of this work by the Natural Sciences and Engineering Research Council of Canada is gratefully acknowledged. We also wish to thank Prof. V. K. Ryabchuk of the State University of St. Petersburg, Russia, for useful discussions.

References and Notes

(1) Serpone, N., Pelizzetti, E., Eds. *Photocatalysis − Fundamentals and Applications*; John Wiley & Sons: New York; 1989.

(2) Fox, M. A.; Dulay, M. T. *Chem. Rev.* **1993**, *93*, 341.

(3) Zamaraev, K. I., Parmon, V. N., Eds. *Photocatalytic Transformation of Solar Energy. Heterogeneous, Homogeneous and Organized Molecular Structures*; Nauka; Novosibirsk, Soviet Union; 1991.

(4) Baru, V. G.; Volkenstein, Th. Th. *The effect of irradiation on surface properties of* semiconductors. Nauka, Moscow, Russia; 1978.

(5) Pelizzetti, E., Schiavello, M., Eds. "*Photochemical Conversion and Storage of Solar Energy*"; Kluwer: Dordrecht; 1991.

(6) Schiavello, M., Ed., *Photocatalysis and Environment. Trends and Applications.*, Kluwer Academic Publisher: Dordrecht, 1987.

(7) Rose, T. L., Conway, B. E., Murphy, O. J., Rudd, E. J., Eds., *Water Purification by Photocatalytic, Photoelectrochemical, and Electrochemical Processes*., The Electrochemical Society, Pennington, N. J., **1994**.

(8) Kamat, P. V. *Chem. Rev.* **1993**, *93*, 267.

(9) Ollis, D. F., Al-Ekabi, H., Eds. "*Photocatalytic and Purification and Treatment of Water and Air*", Elsevier Science, Amsterdam, 1993.

(10) Vilesov Ph. I., Ed., *Uspekhi Photoniki.*, Iss.6., LGU (Leningrad State University), 1977.

(11) Serpone, N.; Salinaro, A. *Pure Appl. Chem.* **1999**, *71*, 303.

(12) Salinaro, A.; Serpone, N.; Emeline, A.; Ryabchuk, V.; Hidaka, H. *Pure Appl. Chem.* **1999**, *71*, 321.

(13) Serpone, N.; Salinaro, A.; Emeline, A. V.; Ryabchuk,V. K. *J. Photochem. Photobiol. A: Chem.* **2000**, *130*, 83.

(14) Basov, L. L.; Kuzmin, G. N.; Prudnikov, I. M.; Solonitsin, Yu. P. *Uspekhi Photoniki.*, Iss.6., Vilesov Th. I., Ed., LGU (Leningrad State University), 1977; pp 82−120.

(15) Emeline, A. V.; Kuzmin, G. N.; Purevdorj, D.; Ryabchuk, V. K.; Serpone, N., *J. Phys. Chem. B* **2000**, *104*, 2989.

(16) Kuznetsov, V. N.; Lisachenko, A. A. *Sov. J. Phys. Chem.* **1991**, *65*, 1568.

(17) Emeline, A. V.; Lobyntseva, E. V.; Ryabchuk, V. K.; Serpone, N. *J. Phys. Chem. B.* **1999**, *103*, 1325.

(18) Sun, L.; Bolton, J. R. *J. Phys. Chem*. **1995**, *99*, 4127.

(19) Serpone, N. *J. Photochem. Photobiol. A: Chem*. **1997**, *104*, 1.

(20) Emeline, A. V.; Rudakova, A. V.; Ryabchuk, V. K.; Serpone, N. *J. Phys. Chem.* **1998**, *102*, 10906.

(21) Emeline, A. V.; Ryabchuk, V. K.; Serpone, N. *J. Photochem. Photobiol. A: Chem*. **2000**, *133*, 89.

(22) Serpone, N.; Sauve, G.; Koch, R.; Tahiri, H.; Pichat, P.; Piccinini, P.; Pelizzetti, E.; Hidaka, H. *J. Photochem. Photobiol. A: Chem.* **1996**, *94*, 191.

(23) Braun, A. M.; Maurette, M.-T.; Oliveros, E. "Photochemical Technology", translated by Ollis, D. F.; Serpone, N.; John Wiley & Sons: Chichester, England, 1991, Chapter 2.

(24) Solonitsin, Yu. P.; Kuzmin, G. N.; Shurigin, F. L.; Yurkin V. M. *Sov. J. Kinet. Catal*. **1976**, *17*, 1267.

(25) Zakharenko, V. S.; Cherkashin, A. E. *React. Kinet. Catal. Lett.* **1983**, 131.

(26) Kuzmin, G. N.; Purevdorj, D.; Shenderovich, I. G. *Russian J. Kinet. Catal*. **1995**, *36*, 790.

(27) Emeline, A. V.; Kuzmin, G. N.; Purevdorj, D.; Shenderovich, I. G. *Russian J. Kinet. Catal*. **1997**, *38*, 446.

(28) Emeline, A. V.; Ryabchuck, V. K.; Serpone, N. *J. Phys. Chem. B* **1999**, *103*, 1316.

(29) Kuzmin, G. N.; Knatko, M. V.; Kurganov, S. V. *React. Kinet. Catal. Lett.* **1983**, *23*, 313.

(30) Ryabchuk, V. K.; Basov, L. L.; Solonitsin, Yu. P. *Sov. J. Chem. Phys.* **1989**, *8*, 1475.

(31) In homogeneous photochemistry, it is well-known that a *unique* quantum yield of a given photochemical process can only be defined under conditions where the rate of that process is independent of substrate concentration, i.e., for a zero-order process. Experimentally this is done for only a few percent conversion of the original substrate (typically for less than 5 to 10%), conditions that also ensure that any intermediates formed do not affect the quantum yield measurement.

(32) Daude, N.; Gout, C.; Jouanin, C. *Phys. Rev. B* **1977**, *15*, 3229.

(33) Bonch-Bruevich, V. L.; Kalashnikov, S. G. *Physics of Semiconductors*, "Nauka", Moscow, Russia; **1990**.

(34) Ross, R. T.; Nozik, A. J. *J. Appl. Phys.* **1982**, *53*, 3813.

(35) Boudreaux, D. S.; Williams, F.; Nozik, A. J. *J. Appl. Phys.* **1980**, *51*, 2158.

(36) Cooper, G.; Turner, J. A.; Parkinson, B. A.; Nozik, A. J. *J. Appl. Phys.* **1983**, *54*, 2158.

(37) Koval, C. A.; Segar, P. R. *J. Am. Chem. Soc.* **1989**, *111*, 2004.

(38) Koval, C. A.; Torres, R. *J. Am. Chem. Soc.* **1993**, *115*, 8368.

(39) Hidaka, H.; Horikoshi, S.; Serpone, N.; Knowland, J. *J. Photochem. Photobiol. A: Chem.* **1997**, *111*, 205.

(40) Warman, J. M.; de Haas, M. P.; Pichat, P.; Serpone, N. *J. Phys. Chem.* **1991**, *95*, 8858.

(41) Enright, B.; Fitzmaurice, D. *J. Phys. Chem*. **1996**, *100*, 1027.

(42) Serpone, N.; Lawless, D.; Khairutdinov, R.; Pelizzetti, E. *J. Phys. Chem.* **1995**, *99*, 16655.

(43) Colombo, D. P., Jr.; Bowman, R. M. *J. Phys. Chem*. **1996**, *100*, 18445, and references therein.

(44) Glassford, K. M.; Chelikowsky, J. R. *Phys. Rev. B* **1992**, *45*, 3874.

(45) Serpone, N.; Lawless, D.; Khairutdinov, R. *J. Phys. Chem.* **1995**, *99*, 16646.

(46) Arntz, F.; Yacoby, Y. *Phys. Rev. Lett*. **1966**, *17*, 857.

(47) Frova, A.; Body, P. J.; Chen, Y. S. *Phys. Rev.* **1967**, *157*, 157.

(48) Kasowski, R. V.; Tait, R. H. *Phys. Rev. B* **1979**, *20*, 5168.

(49) Ye, M., Ph.D. Thesis, University of Notre Dame, Notre Dame, IN, 1989.

(50) Mattews, R. W.; Sangster, D. F. *J. Phys. Chem.* **1965**, *69*, 1938.

(51) Stafford, U.; Gray, K. A.; Kamat, P. V. *J. Phys. Chem.* **1994**, *98*, 6343.

(52) Khairutdinov, R. F.; Burshtein, L. Ya.; Serpone, N. *J. Photochem. Photobiol. A: Chem.* **1996**, *98*, 1.

(53) Khairutdinov, R. F.; Serpone, N. *Prog. React. Kinet*. **1996**, *21*, 1.

(54) Laidler, K. J., "*Chemical Kinetics*", 3rd. ed.; Harper & Row Publ.; New York, 1987, pp 278−281.

(55) Emeline, A. V.; Salinaro, A.; Serpone, N. *J. Photochem. Photobiol. A: Chem*., to be submitted for publication.